Cell Reports

Influenza Vaccination Induces NK-Cell-Mediated Type-II IFN Response that Regulates Humoral Immunity in an IL-6-Dependent Manner

Graphical Abstract

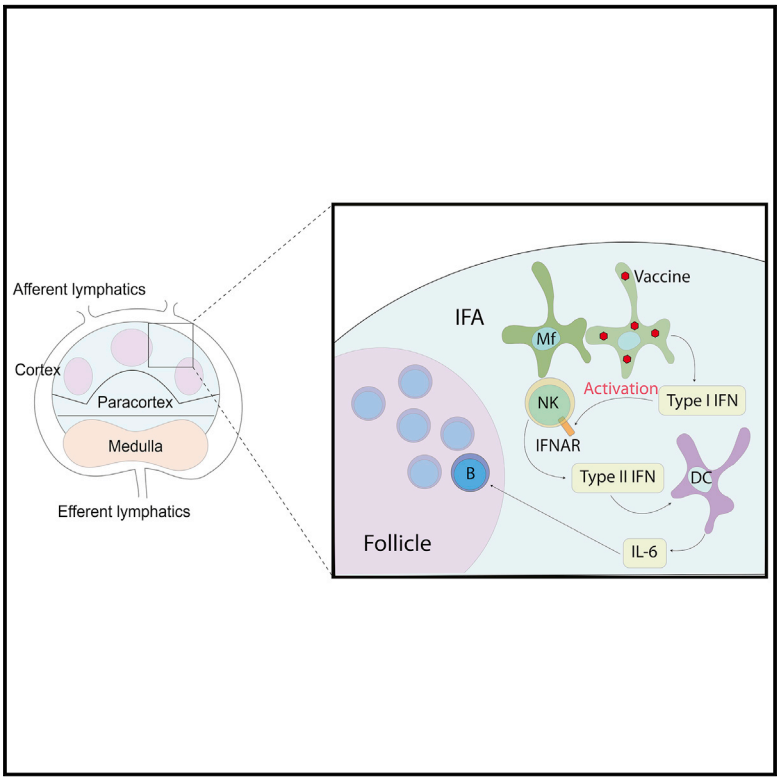

Authors

Yagmur Farsakoglu, Miguel Palomino-Segura, Irene Latino, ..., Federica Sallusto, Jens V. Stein, Santiago F. Gonzalez

Correspondence

santiago.gonzalez@irb.usi.ch

In Brief

The role of natural killer (NK) cells in the context of influenza vaccination is unclear. Farsakoglu et al. demonstrate that NK cells produce early type II IFNs and regulate IL-6 secretion by dendritic cells, which affects the local anti-viral antibody responses in the draining lymph node after influenza vaccination.

Highlights

- NK cells are activated by macrophages in a type-I-IFN-dependent manner
- Early production of IFNγ is mediated by NK cells in the draining lymph node
- NK-cell-secreted IFNγ regulates the recruitment of IL-6+ dendritic cells
- Together IL-6 and IFNγ positively regulate anti-influenza B cell responses

Farsakoglu et al., 2019, Cell Reports *26*, 2307–2315
February 26, 2019
https://doi.org/10.1016/j.celrep.2019.01.104

CellPress

Cell Reports
Report

Influenza Vaccination Induces NK-Cell-Mediated Type-II IFN Response that Regulates Humoral Immunity in an IL-6-Dependent Manner

Yagmur Farsakoglu,[1,2,8] Miguel Palomino-Segura,[1,2] Irene Latino,[1] Silvia Zanaga,[1] Nikolaos Chatziandreou,[1] Diego Ulisse Pizzagalli,[1,3] Andrea Rinaldi,[4] Marco Bolis,[4,5] Federica Sallusto,[1,6] Jens V. Stein,[7] and Santiago F. Gonzalez[1,9,*]

[1]Institute for Research in Biomedicine (IRB), Università della Svizzera italiana, Via Vincenzo Vela 6, 6500 Bellinzona, Switzerland
[2]Graduate School of Cellular and Molecular Sciences, Faculty of Medicine, University of Bern, 3012 Bern, Switzerland
[3]Institute of Computational Science (ICS), Università della Svizzera italiana, Via Giuseppe Buffi 13, 6900 Lugano, Switzerland
[4]Institute of Oncology Research (IOR), Via Vincenzo Vela 6, 6500 Bellinzona, Switzerland
[5]Laboratory of Molecular Biology, Instituto di Ricerche Farmacologiche Mario Negri IRCCS, via Giuseppe La Masa 19, 20156 Milano, Italy
[6]Institute for Microbiology, ETH Zurich, Wolfgang-Pauli-Strasse 10, 8093 Zurich, Switzerland
[7]Theodor Kocher Institute (TKI), University of Bern, Freiestrasse 1, 3000 Bern, Switzerland
[8]Present address: Salk Institute for Biological Studies, La Jolla, CA 92037, USA
[9]Lead Contact
*Correspondence: santiago.gonzalez@irb.usi.ch
https://doi.org/10.1016/j.celrep.2019.01.104

SUMMARY

The role of natural killer (NK) cells in the immune response against vaccines is not fully understood. Here, we examine the function of infiltrated NK cells in the initiation of the inflammatory response triggered by inactivated influenza virus vaccine in the draining lymph node (LN). We observed that, following vaccination, NK cells are recruited to the interfollicular and medullary areas of the LN and become activated by type I interferons (IFNs) produced by LN macrophages. The activation of NK cells leads to their early production of IFNγ, which in turn regulates the recruitment of IL-6+ CD11b+ dendritic cells. Finally, we demonstrate that the interleukin-6 (IL-6)-mediated inflammation is important for the development of an effective humoral response against influenza virus in the draining LN.

INTRODUCTION

While contained inflammation enhances both humoral and cellular adaptive immunity, uncontrolled or persistent inflammation has detrimental roles associated with reduced long-lived memory cell formation and cellular exhaustion (Wherry, 2011). Therefore, it is essential to better understand the mechanisms that lead to the initiation of the inflammatory response following vaccination.

Among the different types of inflammatory molecules, type I interferons (IFNs) are critical for the effective initiation of the inflammatory response and the generation of an antiviral state (Gabay and Kushner, 1999). Additionally, they are also involved in the activation of various immune cells such as dendritic cells (DCs) and natural killer (NK) cells (Madera et al., 2016). In a previous study, we showed that lymph node macrophages (LNMs) are one of the major producers of type I IFNs at early times post influenza vaccination. This mechanism is essential for the activation of DCs and the regulation of the local humoral responses (Chatziandreou et al., 2017). In addition, LNMs activate other innate immune cells involved in the inflammatory process, such as NK cells (Garcia et al., 2012).

NK cells play an important role in eliminating stressed and infected cells without the need for prior sensitization (Vivier et al., 2008). Moreover, they can directly recognize influenza virus via receptor NKp46 (Mendelson et al., 2010). The absence of NKp46 results in increased mortality, highlighting the importance of NK cell functions during influenza infection (Gazit et al., 2006). Previous studies have stressed the role of NK cells as one of the major producers of type II IFNs contributing to the activation of T cells (Martín-Fontecha et al., 2004), macrophages (Mosser and Edwards, 2008), DCs (Gerosa et al., 2002), and B cells (Wilder et al., 1996). Despite the fact that NK cells have been widely studied in various tissue and disease models, their role in response to vaccination needs to be investigated.

RESULTS

NK Cells Are Recruited to the LN and Undergo Type I IFN-Dependent Activation

To assess the involvement of NK cells in response to influenza vaccination at early time points (0–24 h post vaccination; p.v.), we investigated their recruitment to the draining LN after footpad injection of ultraviolet inactivated influenza virus (UVPR8). We observed a significant increase of total NK (Figure 1A) and CD69+ and GranzymeB+ NK cell numbers (Figure 1B) at 12 and 24 h p.v., which correlated with an increase in their fluorescence intensity (Figure 1C). To assess NK cell recruitment, we performed intravital two-photon microscopy (IV-2PM) in combination with epifluorescence time-lapse microscopy using *Ncr1*-GFP mice (Gazit et al., 2006). We observed that NK cells were

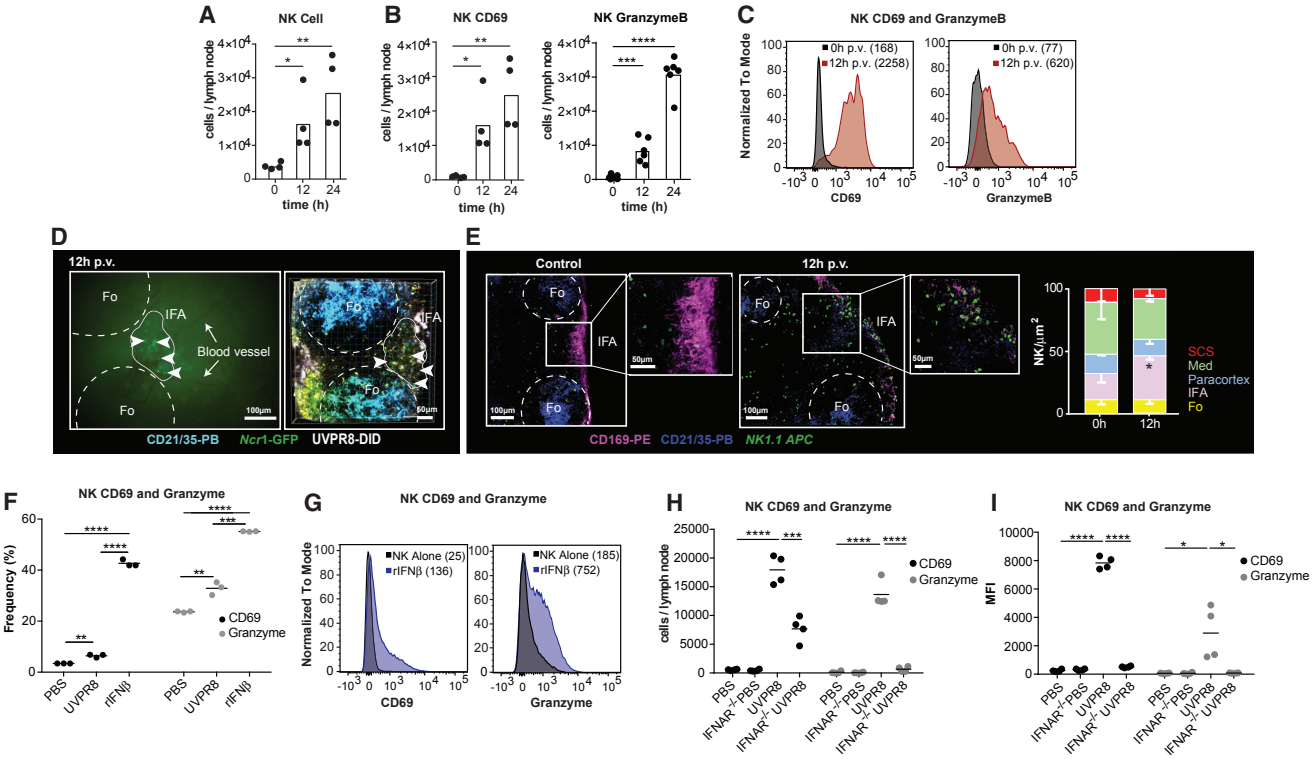

Figure 1. NK Cells Get Recruited to the Popliteal Lymph Node at Early Times after Influenza Vaccination and Are Activated by Type I IFNs

(A and B) Flow cytometry showing total NK (A) and CD69+ and GranzymeB+ NK cell numbers (B) in the lymph node (LN) following vaccination at indicated time points.

(C) Representative histograms of fluorescence intensity showing upregulation of CD69 and GranzymeB at 12 h post vaccination (p.v.) in comparison with non-vaccinated controls. Median fluorescence intensity (MFI) values are indicated in parentheses.

(D) Snapshot from an epifluorescence time lapse (left) and two-photon microscopy (right) showing recruitment of NK cells (green) via blood vessels located in the interfollicular area (IFA) of the LN at 12 h p.v.

(E) Confocal micrographs showing recruitment of NK cells in the IFA of LN from control (left) and vaccinated at 12 h p.v. (middle). The right graph shows the quantification of the frequency of NK cell density in the medullary (Med), IFA, cortex, follicle (Fo), and subcapsular sinus (SCS) areas of the LN at indicated time points.

(F) Flow cytometry showing frequency of CD69+ and GranzymeB+ NK cells after 12 h culture with UVPR8 and/or recombinant IFN-β compared with control group.

(G) Representative histograms of fluorescence intensity rIFN-β-treated NK cells showing upregulation of CD69 and GranzymeB at 12 h p.v. compared to control groups. MFIs are indicated in parentheses.

(H and I) Flow cytometry showing total CD69+ NK and GranzymeB+ NK cell numbers (H) and MFI values (I) at 12 h p.v. in LN of IFNAR$^{-/-}$ and B6 mice.

In all figures, the presented data are representative of at least three independent experiments. Results are given as mean ± SD. ns, not significant, $p > 0.05$; *$p < 0.05$; **$p < 0.01$; ***$p < 0.001$; ****$p < 0.0001$.

recruited via blood vessels (Figure 1D, left; Video S1) and accumulated in the interfollicular area (IFA) of the LN (Figure 1D, right). Additionally, using immunohistochemistry, we confirmed a significant increase of these cells in the IFA of the LN at 12 h p.v. (Figure 1E).

Next, we assessed the mechanism by which NK cells are recruited to the LN by evaluating their number in IL1R$^{-/-}$, interferon-α/β receptor (IFNAR)$^{-/-}$, and CXCR3$^{-/-}$ animals. We observed that IL1R$^{-/-}$, IFNAR$^{-/-}$, CXCR3$^{-/-}$ showed no reduction in the total number of NK cells in the LN at 12 h p.v. (Figures S1A and S1B). However, we observed that LN macrophages were involved in the recruitment of the NK cells as their depletion with clodronate liposomes (CLLs) significantly reduced the number of NK cells at 12 h p.v. (Figure S1C).

NK cells can directly recognize hemagglutinin (HA) from influenza virus via receptor NKp46 (Mandelboim et al., 2001). Thus, we tested whether influenza vaccine can directly activate NK cells *in vitro*. We cultured spleen-sorted NK cells with UVPR8 and observed a partial activation at 12 h post-culture, indicated by a significant increase of CD69+ and GranzymeB+ NK cell frequency (Figure 1F). Next, we cultured NK cells in the presence or absence of recombinant IFN-β (rIFN-β). As expected, rIFN-β alone was enough to increase the CD69+ and GranzymeB+ NK cell frequency (Figure 1F), along with their expression (Figure 1G). Moreover, we observed that the numbers of CD69+ and GranzymeB+ NK cells decreased significantly in IFNAR$^{-/-}$ mice at 12 h p.v. (Figure 1H) in concordance with the reduced median fluorescence intensity (MFI) (Figure 1I). Finally, to

evaluate if the recruitment of activated NK cells at 12 h p.v. was influenza specific, we designed a similar set of experiments using UV-inactivated DNA virus (vaccinia UVNYVAC-C). Interestingly, we observed that the immunization with vaccinia promoted a stronger NK cell recruitment at 12 h p.v. (Figure S1D). Additionally, we observed a significant increase in the total number of CD69+ and IFNγ+ NK cells (Figures S1E and S1G, respectively) but not in the MFI levels of CD69 and GranzymeB, which were significantly reduced in animals vaccinated with vaccinia compared with influenza (Figures S1E and S1F, respectively).

Subcapsular Sinus and Medullary Macrophages Interact with NK Cells, Leading to Their Activation

To study the interaction between NK cells and LNMs, we performed IV-2PM at 12 h p.v. on the popliteal LN of *Ncr1*-GFP mice. We observed that NK cells interact with both subcapsular sinus macrophages (SSMs; CD169+, F4/80−; Figure 2A; Video S2) and medullary macrophages (MMs; CD169+, F4/80+; Figure 2B, Video S2). To further evaluate these interactions, we analyzed NK cell motion tracks in different regions of the LN. We found that the preferential direction of NK cells was higher in the IFA and the medulla compared to the subcapsular sinus area (SCS; Figure 2C). Moreover, NK cells moved slower in the medulla and SCS in comparison to the IFA, as indicated by the reduction in their mean track speed (Figure 2D). Analysis of the arrest coefficient, defined as the proportion of time in which an NK cell moves slower than 2 μm/min, demonstrated that NK cells arrested at a significantly higher rate in the medulla compared to the SCS and the IFA (Figure 2E). To evaluate the ability of LNMs to stimulate and activate NK cells *in vivo*, we eliminated LNMs by treatment with CLLs and analyzed the expression of CD11b by NK cells, as a marker of their maturation (Kim et al., 2002). We observed that CLL-treated mice had a significantly lower frequency of mature NK cells at 12 h p.v. in comparison to the CLL-untreated group (Figure 2F). In addition, the MFI levels of CD69 and GranzymeB in NK cells were significantly reduced in the CLL-treated group compared to control groups (Figure 2G), confirming the involvement of LNMs in NK cell activation.

Involvement of NK Cells in the Early Inflammatory Reaction Initiated by LNMs

Considering that NK cells are known to be one of the key players in the type II IFN response (Vivier et al., 2008), we evaluated their production of IFNγ following influenza vaccination. The analysis of LN extracts from the first 24 h following vaccination showed a prominent peak in IFNγ levels at 12 h p.v., followed by a striking reduction at 24 h p.v. (Figure 3A). We observed that the number IFNγ+ NK cells peaked at 12 h p.v. (Figure 3B), correlating with their frequency (Figure 3C). Moreover, we confirmed that NK cells were the major producers of IFNγ at this time (Figures S2A and S2B) and pre-treatment with the αNK1.1 significantly lowered the IFNγ levels in the LN (Figure 3D). In addition, confocal microscopy revealed that IFNγ+ NK cells were located in the IFA of the LN at 12 h p.v. (Figure 3E). Having identified the effect of LNMs on NK cell activation, we observed a close interaction between IFNγ+ cells and CD169+ macrophages at 12 h p.v. using IV-2PM imaging (Figure 3F). We assessed the involvement of LNMs in NK cell production of IFNγ by depleting LNMs with CLLs. We detected a significant decrease in IFNγ+ NK cell numbers in animals lacking LNMs (Figure 3G), which correlated with a significant reduction of secreted IFNγ at 12 h p.v. (Figure 3H). We further evaluated the effect of IFNAR on the production of IFNγ by NK cells. We found that the total number of IFNγ+ NK cells (Figure 3I) and their MFI (Figure 3J) were significantly reduced in IFNAR$^{-/-}$ mice compared to the control group. To further evaluate the role of NK cells in the induction of the inflammatory response, we performed real-time PCR on samples obtained from mice depleted of NK cells in comparison to the control group. We observed that the transcription levels of the inflammatory mediators IFNγ and IL-6 were significantly elevated at 12 h p.v. in comparison to PBS controls and NK-cell-depleted mice (Figures 3K and 3L). In contrast, IL-18 and IL-1β levels were increased in mice lacking NK cells (Figures 3M and 3N).

Early IFNγ Secreted by NK Cells Is Important for the Local Production of IL-6 in the Draining LN

To confirm that the reduction of IL-6 transcripts correlated with its protein level, we measured the concentration of IL-6 in NK-cell-depleted mice in comparison to the control group. We confirmed that the absence of NK cells significantly reduced the levels of IL-6 in the draining LN (Figure 4A). Interestingly, we observed that the reduction of IL-6 was dependent on IFNγ (Figure 4A). Having shown the effects of LNMs and type I IFNs on the regulation of IFNγ production by NK cells, we examined the levels of IL-6 in CD169^{DTR} and IFNAR$^{-/-}$ mice at 12 h p.v. We observed a prominent reduction in the levels of IL-6 (Figure 4B) in animals lacking LNMs or type I IFN signaling. Moreover, in concordance with earlier studies (Hunter and Jones, 2015), we found that IL-6 production was dependent on MyD88 signaling, as MyD88$^{-/-}$ mice exhibited a complete reduction in secreted IL-6 at 12 h p.v. (Figure 4C). Using flow cytometry, we identified CD11b+ DCs as the major source of IL-6 at 12 h p.v. (Figures 4D and 4E). To investigate whether IFNγ produced by NK cells is involved either in the proliferation or recruitment of CD11b+ DCs, we checked their Ki-67 expression in the presence or absence of NK cells at 12 h p.v. The absence of NK cells did not affect DC proliferation (Figure S3A). However, we measured a significant decrease in the number of IL-6+ CD11b+ DCs when we eliminated NK cells or blocked IFNγ signaling (Figures 4F and 4G, respectively). Additionally, we could observe a decrease in the levels of different chemokines known to be involved in the recruitment of DC precursors to the LN (Figures S3B–S3D). Furthermore, to evaluate the capacity of IFNγ to directly stimulate IL-6 production by CD11b+ DCs, we sorted CD11b+ splenic DCs and stimulated them with recombinant IFNγ or lipopolysaccharides (LPS) for 12 h. We saw that IFNγ could directly act on CD11b+ DCs to induce IL-6 secretion (Figure S3E).

IL-6 Production Regulates Humoral Immunity in the Draining LN

To determine whether additional production of IL-6 occurs at later time points p.v., we examined the kinetics of IL-6 secretion in the LN in response to UVPR8. We observed that the peaks of

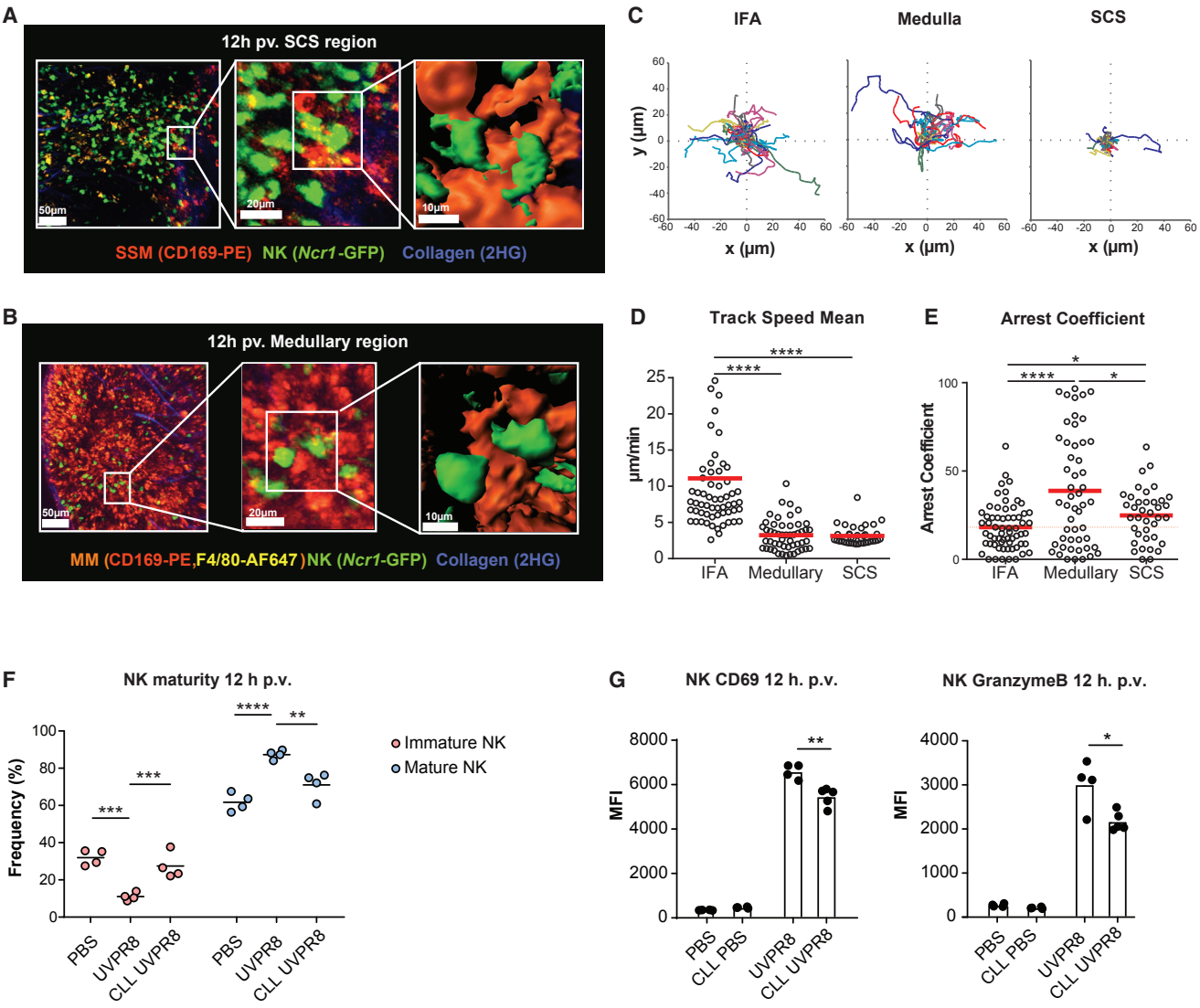

Figure 2. Subcapsular Sinus and Medullary Macrophages Interact Differently with NK, Leading to Their Activation

(A and B) Representative intravital two-photon micrograph showing close interactions between infiltrated NK cells with subcapsular sinus macrophages (SSMs) (CD169-PE) (A) and medullary macrophages (MMs; CD169-PE, F4/80-AF647) (B) in the LN at 12 h p.v. Central panels represent the magnified dotted box. Right panels demonstrated surface reconstruction of the zoomed images.

(C) Graphical representation of tracks with common origin showing preferential direction of NK cells in the interfollicular (IFA), medullary, and subcapsular sinus area (SCS).

(D and E) Representative graphs showing track speed mean (D) and arrest coefficient (E) of NK cells in the indicated regions of the LN at 12 h p.v.

(F) Flow cytometric analysis of the frequency of CD11b+ and CD11b− NK cells at 12 h p.v. in mice treated with/without CLLs compared with PBS controls.

(G) Flow cytometric quantification of CD69+ and GranzymeB+ NK cells at 12 h p.v. in mice treated with/without CLLs compared with PBS controls.

In all figures, the presented data are representative of at least three independent experiments. Results are given as mean ± SD. ns, $p > 0.05$; *$p < 0.05$; **$p < 0.01$; ***$p < 0.001$; ****$p < 0.0001$.

IL-6 and IFNγ occur within the first 24 h p.v. (Figures 5A and 5B, respectively). Previous studies have demonstrated that IL-6 affects B cell responses (Eto et al., 2011). Therefore, to examine the involvement of IL-6 in the regulation of the local humoral responses to influenza vaccine, we neutralized the initial IL-6 production by administrating αIL-6 antibodies at the time of vaccination. Using enzyme-linked immunospot assay (ELISPOT) analysis, we observed a significant reduction in the number of influenza-specific antibody-secreting cells (ASCs) in the draining LN at day 10 p.v. in IL-6-neutralized mice compared to untreated controls (Figure 5C). Next, we tested whether the elimination of NK cells or the absence of the interferon-g (IFNgR) would result in a reduction of the local B cell responses to the virus. ELISPOT analysis confirmed that the number of influenza-specific ASCs were significantly reduced in both cases, compared to the respective control groups (Figures 5D and 5E). Having validated

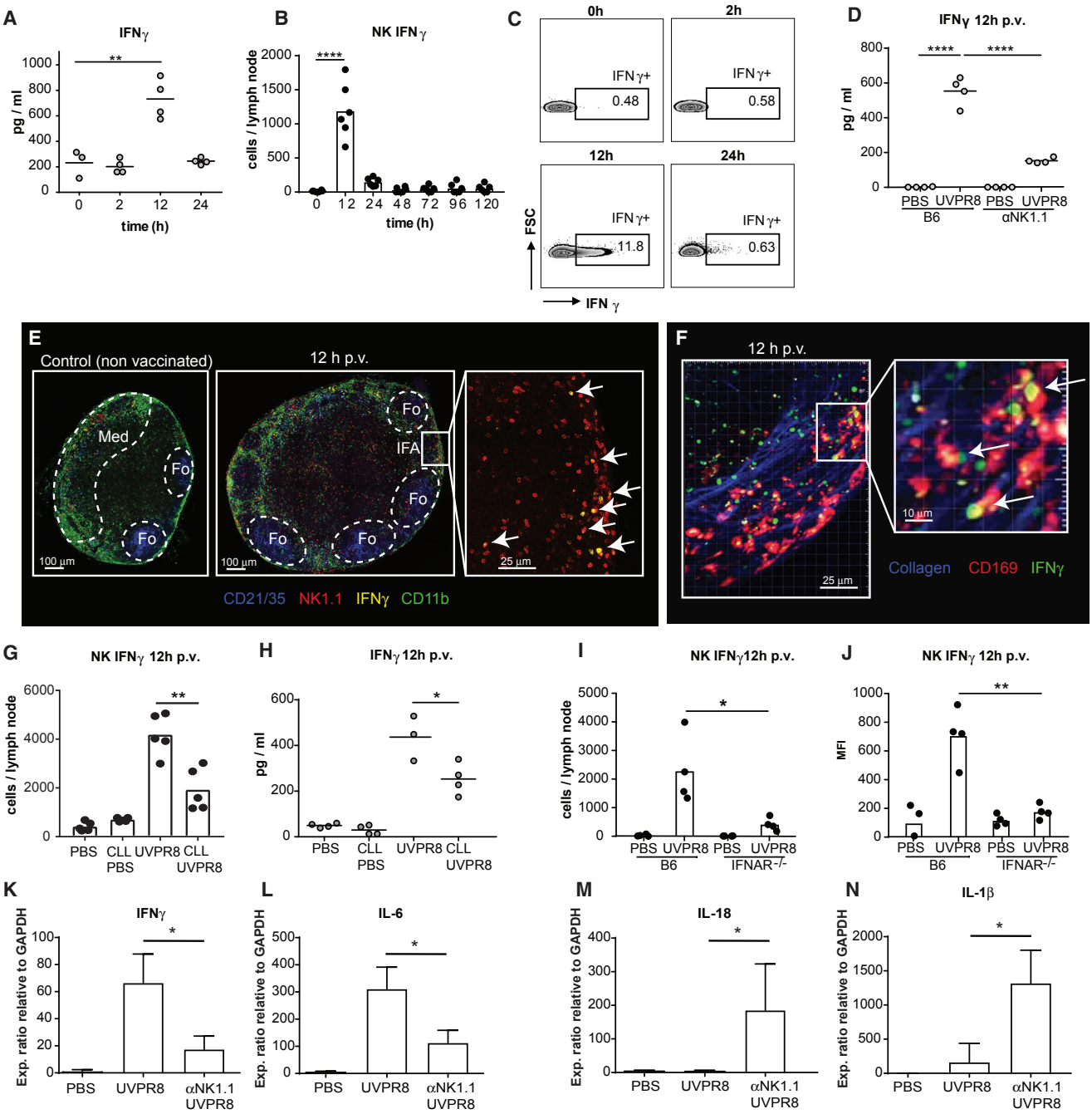

Figure 3. Early Production of IFNγ by NK Cells Is Dependent on the Type I IFN Response Initiated by LNMs

(A) ELISA showing IFNγ in the LN at indicated time points p.v.

(B and C) Flow cytometric analysis of total IFNγ+ NK cell numbers (B) and representative plots showing frequency of IFNγ+ NK cells (C) at indicated time points p.v.

(D) Cytoplex indicating IFNγ in LN of αNK1.1-treated mice and control groups at 12 h p.v.

(E) Representative confocal micrograph of popliteal LN at 12 h p.v. (middle) showing IFNγ+ cells (yellow), NK1.1+ cells (red), and IFNγ-producing NK cells (merge) located in the interfollicular area (IFA) of the LN. The left panel represent the control group, and the right panel indicates the zoomed area. Arrows indicate IFNγ+ NK cells at 12 h p.v.

(F) Representative micrograph (left) and amplification (right) showing close interactions between IFNγ+ cells and LN macrophages (CD169-PE) at 12 h p.v. White arrows indicate IFNγ+ cells.

(G) Flow cytometry showing IFNγ+ NK total numbers at 12 h p.v. in CLL-treated mice with respect to the control group.

(H) Cytoplex showing a reduction of IFNγ levels in LN of CLL-treated mice at 12 h p.v. compared to control groups.

(legend continued on next page)

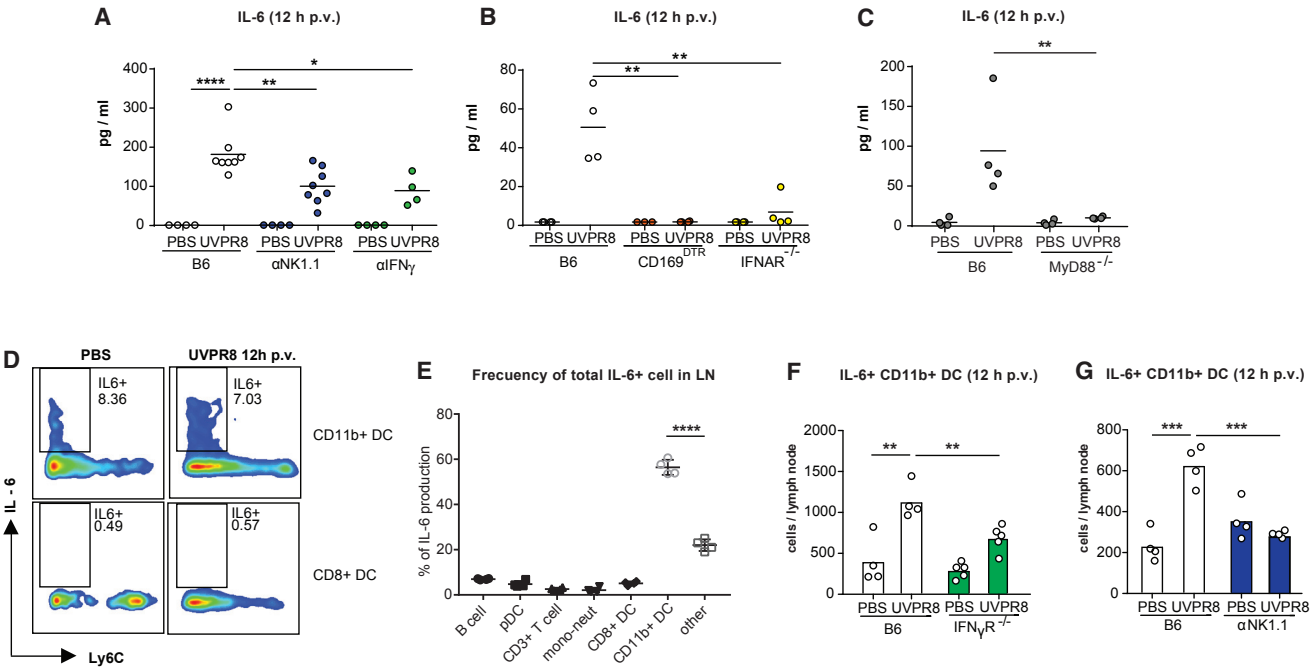

Figure 4. NK Cells Regulate DC Production of IL-6

(A) Cytoplex analysis of IL-6 in popliteal LN from anti-NK1.1-treated and anti-IFNγ-treated mice compared to the control group at 12 h p.v.

(B and C) Cytoplex analysis of IL-6 in popliteal LN $CD169^{DTR}$, $IFNAR^{-/-}$ (B), and $MyD88^{-/-}$ (C) mice compared to the control group at 12 h p.v.

(D) Representative flow cytometry indicating IL-6 production of CD11b+ DCs and CD8+ DCs at 12 h p.v. compared to control.

(E) Flow cytometry showing the frequency of the IL-6+ cells in the LN.

(F and G) Flow cytometry indicating IL-6+ DC numbers at 12 h p.v. in LN of $IFN\gamma R^{-/-}$ (F) and anti-NK1.1-treated mice (G).

In all figures, the presented data are representative of at least three independent experiments. Results are given as mean ± SD. ns, $p > 0.05$; *$p < 0.05$; **$p < 0.01$; ***$p < 0.001$; ****$p < 0.0001$.

the importance of IFNγ and IL-6 in driving influenza-specific humoral response, we investigated whether immunoglobulin G (IgG) ASC reduction was due to impairment in B cell development. We found that, while the level of IgG antibodies was reduced, germinal center and plasma cell numbers were not altered using neutralizing antibody treatments or when the type II IFN signaling was blocked ($IFN\gamma R^{-/-}$) at 12 h p.v. (Figures S4A and S4B).

DISCUSSION

In this study, we revealed that following influenza vaccination, NK cells are preferentially located at the interfollicular and medullary regions of the LN, which is in accordance with a previous report (Bajénoff et al., 2006). Additionally, we demonstrated that NK cell recruitment was independent of CXCR3 and dependent on the presence LNMs. We also demonstrated that neither type I IFNs nor IL-1α, produced by LNMs after vaccination (Chatziandreou et al., 2017), were involved in the initial recruitment of NK cells. It is possible that the release of other danger signals after the necrotic death of the LNMs (Chatziandreou et al., 2017) could be involved in the recruitment of NK cells. Former studies outlined that the activation of NK cells was associated with their interaction with SSMs (Coombes et al., 2012; Garcia et al., 2012). We show that MMs also interact with NK cells, forming stable contacts in the medullary area. Considering the role of type I IFNs on the functions of NK cells (Madera et al., 2016), we confirmed that IFN signaling was necessary for the effective activation of NK cells. In a previous work, we reported that LNMs are responsible for the initial production of type I IFNs following influenza vaccination (Chatziandreou et al., 2017), which could explain the close interactions of NK cells with the LNMs in these areas. We also saw that recruitment of NK cells in the IFA, together with their high speed, correlates with the presence of IFNγ+ cells in this region. In fact, we have formerly shown that IFA are one of the major sites for type I IFN production (Chatziandreou et al., 2017). NK cells require several cytokines for full maturation and to perform their effector functions (Brady et al.,

(I and J) Flow cytometry of IFNγ+ NK total numbers (I) and MFI values (J) in $IFNAR^{-/-}$ and control mice at 12 h p.v.

(K–N) Quantitative real-time PCR analysis of cDNA from LN of mice treated with/without anti NK1.1 compared to controls at 12 h p.v. testing the expression of inflammatory molecules IFNγ (K), IL-6 (L), IL-18 (M), and IL-1β (N).

In all figures, the presented data are representative of at least three independent experiments. Results are given as mean ± SD. ns, $p > 0.05$; *$p < 0.05$; **$p < 0.01$; ****$p < 0.0001$.

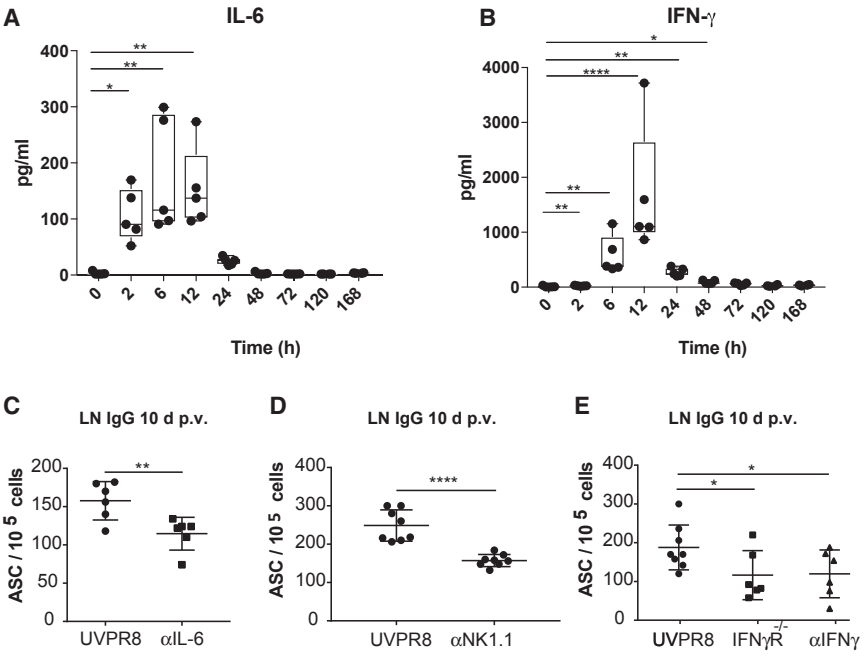

Figure 5. NK-Regulated IL-6 Production Is Involved in the Humoral Response against Influenza Vaccine

(A and B) Time course showing the secreted levels of the cytokines IL-6 (A) and IFNγ (B) in the LN at 2, 6, 12, 24, 48, 72, 120, and 168 h p.v.

(C–E) ELISPOT analysis of IgG antibody-secreting cells (ASCs) from UVPR8-vaccinated, αIL-6-treated (C), αNK1.1-treated (D), and IFNγR$^{-/-}$-treated and αIFNγ-treated (E) mice at 10 days p.v. In all figures, the presented data are representative of at least three independent experiments. Results are given as mean ± SD. ns, $p > 0.05$; *$p < 0.05$; **$p < 0.01$; ****$p < 0.0001$.

2010). The decrease of NK cell maturation, activation, and production of IFNγ observed in the interferon-α/β receptor knockout (IFNARKO) mice could be associated with the early production of this cytokine by the LNMs. However, we cannot exclude the contribution of other type-I-IFN-producing cells or alternative factors that might affect NK cell effector functions.

It was demonstrated that innate CD8+ T cells are the major producers of early IFNγ after administration of modified vaccinia virus (MVA) in the LN (Kastenmüller et al., 2012). However, we showed that following influenza vaccination, early production of IFNγ was mediated by NK cells. The observed discrepancy is most likely related to the type of pathogen studied, since vaccination with another attenuated vaccinia virus (NYVAC-C) showed that the magnitude of NK cell recruitment and their effector functions were different in both models. Further, MVA was shown to activate the inflammasome pathway, yet we could not detect the expression of inflammasome-associated molecules in our model. Interestingly, depletion of NK cells resulted in increased transcription of IL-18 and IL-1β, which might be related with the absence of IFNγ as it was previously shown that IFNγ promotes the production of nitric oxide (NO) that prevents inflammasome assembly (Mao et al., 2013; Mishra et al., 2013).

Previous studies have described that IFNγ produced by NK cells is essential for Th1 differentiation (Martín-Fontecha et al., 2004). Prior to differentiation, CD4+ T cells need to be primed by DCs in a multi-step process that requires at least a day (Mempel et al., 2004). Although we observed an earlier release of IFNγ at 2 h p.v., the peak of IFNγ secretion occurred at 12 h p.v.; therefore, we discarded involvement of early IFNγ in Th1 differentiation. Instead, IFNγ is also known to regulate the production of various pro-inflammatory mediators, including tumor necrosis factor alpha (TNF-α) (Donnelly et al., 1995), IL-12 (Libraty et al., 1997), and IL-6 (Yi et al., 1996). In fact, the peaks of IFNγ and IL-6 secretion coincided, and both transcript and protein levels of IL-6 were reduced in mice lacking NK cells. Further, the 2 h IFNγ release also correlated with the presence of IL-6, confirming the interdependence of the two cytokines. Importantly, neutralization of IFNγ resulted in decreased IL-6 secretion. It is important to mention that a prominent decrease in IL-6 levels observed in mice lacking type I IFN receptors or LNMs suggests the presence of additional factors in its regulation besides NK-cell-secreted IFNγ. Among the various types of IL-6-producing cells (Hunter and Jones, 2015), we revealed that CD11b+ DCs were the major source of this cytokine at 12 h p.v. Moreover, we confirmed that IFNγ can act directly on a CD11b+ DC population to induce the secretion of IL-6, as well as contributing to their recruitment. Also, in accordance with previous studies (Naugler et al., 2007), the production of IL-6 was dependent on viral recognition by Toll-like receptors, as the absence of MyD88 signaling abolished its secretion. Interestingly, we show that the lack of NK cells or IFNγ reduced the total number of IL-6-producing DCs, which could be associated with poor monocyte differentiation into DCs caused by the absence of IFNγ (Goldszmid et al., 2012). Moreover, proliferation of IL-6+ DCs was not affected by the absence of NK cells, suggesting that the decrease is also not related with the proliferative capacity of DCs. In fact, it is known that IFNγ is essential for DC homeostasis and activation (Akbar et al., 1996). Therefore, it is possible that NK cell depletion affects the reciprocal interactions between DCs and NK cells required for DC homeostasis (Gerosa et al., 2002), leading to the observed reduction in the number of DCs. Along this line, depletion of NK cells resulted in decreased levels of macrophage inflammatory protein (MIP)-1α, which is known to affect CD8a− CD11b+ DC maturation and activation in the LN (Bachmann et al., 2006; Trifilo and Lane, 2004). Hence, it is probable that NK cells are involved in activating DCs for IL-6 production along with their maintenance in the LN at 12 h post influenza vaccination.

We showed that the initial inflammatory peak directly affects the humoral response to influenza virus, as blocking IL-6 reduced influenza-specific ASCs in the draining LN. The mechanism by which IL-6 might influence this response is most likely

related with the regulation of the follicular helper T cells (T_{FH}) differentiation and B cell activity as previously described (Choi et al., 2013; Eto et al., 2011). Further, elimination of NK cells, hence IFNγ, may skew the overall inflammatory response, which can affect the antibody isotype class switching, leading to a reduction in IgG levels. It should also be noted that the depletion method used here also depletes natural killer T (NKT) cells. Although, we have shown that NKT cells are not involved in the initial IFNγ secretion and that we do not detect the presence of IL-4 (Chatziandreou et al., 2017) in our vaccination model, it is possible that elimination of NKT cells affects the overall B cell responses by other means.

In this work, we show that the type I IFN response generated by LNMs is associated with the activation of NK cells, which in turn produce IFNγ leading to the recruitment of IL-6+ CD11b+ DCs. We demonstrated that both IL-6 and type II IFNs regulate the influenza-specific local B cell responses.

STAR★METHODS

Detailed methods are provided in the online version of this paper and include the following:

- KEY RESOURCES TABLE
- CONTACT FOR REAGENT AND RESOURCE SHARING
- EXPERIMENTAL MODEL AND SUBJECT DETAILS
  - Mice
  - *In vitro* NK cell culture and IFN-β stimulation
  - *In vitro* CD11b+ DC culture and IFNγ stimulation
- METHOD DETAILS
  - Virus production, inactivation and labeling
  - Antigen administration and injections
  - Flow cytometry
  - Immunohistology/microscopy
  - Cytoplex assay
  - ELISPOT
  - Multiphoton microscopy and analysis
  - qPCR
- QUANTIFICATION AND STATISTICAL ANALYSIS
  - Statistics

SUPPLEMENTAL INFORMATION

Supplemental Information can be found with this article online at https://doi.org/10.1016/j.celrep.2019.01.104.

ACKNOWLEDGMENTS

We thank Prof. M. Thelen, Prof. A. Jaworowski, and Dr. J. Abe for valuable discussions. We thank Prof. M. Esteban for providing vaccinia virus NYVAC-C, F. Thelen, D. Jarrossay, and R. D'Antuono for technical support, and Prof. Br. Horvat for providing $CD169^{DTR}$ mice. This work was supported by the Swiss National Science Foundation (SNF) grants 176124, R'Equip (145038), and Ambizione (148183) and a Marie Curie Reintegration Grant (612742).

AUTHOR CONTRIBUTIONS

S.F.G. directed the study. S.F.G., Y.F., M.P.-S., and I.L. designed experiments, analyzed and interpreted the results, and wrote the manuscript. Y.F., M.P.-S., I.L., S.Z., N.C., and A.R. performed experiments. D.U.P. and M.B. analyzed and interpreted results. F.S. and J.V.S. interpreted results and provided reagents.

DECLARATION OF INTERESTS

All the authors declare no competing financial interests.

Received: February 6, 2018
Revised: December 11, 2018
Accepted: January 28, 2019
Published: February 26, 2019

REFERENCES

Akbar, S.M., Inaba, K., and Onji, M. (1996). Upregulation of MHC class II antigen on dendritic cells from hepatitis B virus transgenic mice by interferon-gamma: abrogation of immune response defect to a T-cell-dependent antigen. Immunology *87*, 519–527.

Bachmann, M.F., Kopf, M., and Marsland, B.J. (2006). Chemokines: more than just road signs. Nat. Rev. Immunol. *6*, 159–164.

Bajénoff, M., Breart, B., Huang, A.Y., Qi, H., Cazareth, J., Braud, V.M., Germain, R.N., and Glaichenhaus, N. (2006). Natural killer cell behavior in lymph nodes revealed by static and real-time imaging. J. Exp. Med. *203*, 619–631.

Barnden, M.J., Allison, J., Heath, W.R., and Carbone, F.R. (1998). Defective TCR expression in transgenic mice constructed using cDNA-based α- and β-chain genes under the control of heterologous regulatory elements. Immunol. Cell Biol. *76*, 34–40.

Brady, J., Carotta, S., Thong, R.P., Chan, C.J., Hayakawa, Y., Smyth, M.J., and Nutt, S.L. (2010). The interactions of multiple cytokines control NK cell maturation. J. Immunol. *185*, 6679–6688.

Chatziandreou, N., Farsakoglu, Y., Palomino-Segura, M., D'Antuono, R., Pizzagalli, D.U., Sallusto, F., Lukacs-Kornek, V., Uguccioni, M., Corti, D., Turley, S.J., et al. (2017). Macrophage Death following Influenza Vaccination Initiates the Inflammatory Response that Promotes Dendritic Cell Function in the Draining Lymph Node. Cell Rep. *18*, 2427–2440.

Choi, Y.S., Eto, D., Yang, J.A., Lao, C., and Crotty, S. (2013). Cutting edge: STAT1 is required for IL-6-mediated Bcl6 induction for early follicular helper cell differentiation. J. Immunol. *190*, 3049–3053.

Coombes, J.L., Han, S.-J., van Rooijen, N., Raulet, D.H., and Robey, E.A. (2012). Infection-induced regulation of natural killer cells by macrophages and collagen at the lymph node subcapsular sinus. Cell Rep. *2*, 124–135.

Donnelly, R.P., Freeman, S.L., and Hayes, M.P. (1995). Inhibition of IL-10 expression by IFN-gamma up-regulates transcription of TNF-alpha in human monocytes. J. Immunol. *155*, 1420–1427.

Eto, D., Lao, C., DiToro, D., Barnett, B., Escobar, T.C., Kageyama, R., Yusuf, I., and Crotty, S. (2011). IL-21 and IL-6 are critical for different aspects of B cell immunity and redundantly induce optimal follicular helper CD4 T cell (Tfh) differentiation. PLoS ONE *6*, e17739.

Gabay, C., and Kushner, I. (1999). Acute-phase proteins and other systemic responses to inflammation. N. Engl. J. Med. *340*, 448–454.

Garcia, Z., Lemaître, F., van Rooijen, N., Albert, M.L., Levy, Y., Schwartz, O., and Bousso, P. (2012). Subcapsular sinus macrophages promote NK cell accumulation and activation in response to lymph-borne viral particles. Blood *120*, 4744–4750.

Gazit, R., Gruda, R., Elboim, M., Arnon, T.I., Katz, G., Achdout, H., Hanna, J., Qimron, U., Landau, G., Greenbaum, E., et al. (2006). Lethal influenza infection in the absence of the natural killer cell receptor gene Ncr1. Nat. Immunol. *7*, 517–523.

Gerosa, F., Baldani-Guerra, B., Nisii, C., Marchesini, V., Carra, G., and Trinchieri, G. (2002). Reciprocal activating interaction between natural killer cells and dendritic cells. J. Exp. Med. *195*, 327–333.

Glaccum, M.B., Stocking, K.L., Charrier, K., Smith, J.L., Willis, C.R., Maliszewski, C., Livingston, D.J., Peschon, J.J., and Morrissey, P.J. (1997). Phenotypic

and functional characterization of mice that lack the type I receptor for IL-1. J. Immunol. *159*, 3364–3371.

Goldszmid, R.S., Caspar, P., Rivollier, A., White, S., Dzutsev, A., Hieny, S., Kelsall, B., Trinchieri, G., and Sher, A. (2012). NK cell-derived interferon-γ orchestrates cellular dynamics and the differentiation of monocytes into dendritic cells at the site of infection. Immunity *36*, 1047–1059.

Gómez, C.E., Nájera, J.L., Jiménez, V., Bieler, K., Wild, J., Kostic, L., Heidari, S., Chen, M., Frachette, M.-J., Pantaleo, G., et al. (2007). Generation and immunogenicity of novel HIV/AIDS vaccine candidates targeting HIV-1 Env/Gag-Pol-Nef antigens of clade C. Vaccine *25*, 1969–1992.

Gonzalez, S.F., Lukacs-Kornek, V., Kuligowski, M.P., Pitcher, L.A., Degn, S.E., Kim, Y.-A., Cloninger, M.J., Martinez-Pomares, L., Gordon, S., Turley, S.J., and Carroll, M.C. (2010). Capture of influenza by medullary dendritic cells via SIGN-R1 is essential for humoral immunity in draining lymph nodes. Nat. Immunol. *11*, 427–434.

Hancock, W.W., Lu, B., Gao, W., Csizmadia, V., Faia, K., King, J.A., Smiley, S.T., Ling, M., Gerard, N.P., and Gerard, C. (2000). Requirement of the chemokine receptor CXCR3 for acute allograft rejection. J. Exp. Med. *192*, 1515–1520.

Huang, S., Hendriks, W., Althage, A., Hemmi, S., Bluethmann, H., Kamijo, R., Vilcek, J., Zinkernagel, R., and Aguet, M. (1993). Immune response in mice that lack the interferon-g receptor. Science *260*, 1742–1744.

Hunter, C.A., and Jones, S.A. (2015). IL-6 as a keystone cytokine in health and disease. Nat. Immunol. *16*, 448–457.

Kastenmüller, W., Torabi-Parizi, P., Subramanian, N., Lämmermann, T., and Germain, R.N. (2012). A spatially-organized multicellular innate immune response in lymph nodes limits systemic pathogen spread. Cell *150*, 1235–1248.

Kim, S., Iizuka, K., Kang, H.-S.P., Dokun, A., French, A.R., Greco, S., and Yokoyama, W.M. (2002). In vivo developmental stages in murine natural killer cell maturation. Nat. Immunol. *3*, 523–528.

Libraty, D.H., Airan, L.E., Uyemura, K., Jullien, D., Spellberg, B., Rea, T.H., and Modlin, R.L. (1997). Interferon-gamma differentially regulates interleukin-12 and interleukin-10 production in leprosy. J. Clin. Invest. *99*, 336–341.

Madera, S., Rapp, M., Firth, M.A., Beilke, J.N., Lanier, L.L., and Sun, J.C. (2016). Type I IFN promotes NK cell expansion during viral infection by protecting NK cells against fratricide. J. Exp. Med. *213*, 225–233.

Mandelboim, O., Lieberman, N., Lev, M., Paul, L., Arnon, T.I., Bushkin, Y., Davis, D.M., Strominger, J.L., Yewdell, J.W., and Porgador, A. (2001). Recognition of haemagglutinins on virus-infected cells by NKp46 activates lysis by human NK cells. Nature *409*, 1055–1060.

Mao, K., Chen, S., Chen, M., Ma, Y., Wang, Y., Huang, B., He, Z., Zeng, Y., Hu, Y., Sun, S., et al. (2013). Nitric oxide suppresses NLRP3 inflammasome activation and protects against LPS-induced septic shock. Cell Res. *23*, 201–212.

Martín-Fontecha, A., Thomsen, L.L., Brett, S., Gerard, C., Lipp, M., Lanzavecchia, A., and Sallusto, F. (2004). Induced recruitment of NK cells to lymph nodes provides IFN-γ for T(H)1 priming. Nat. Immunol. *5*, 1260–1265.

Mempel, T.R., Henrickson, S.E., and Von Andrian, U.H. (2004). T-cell priming by dendritic cells in lymph nodes occurs in three distinct phases. Nature *427*, 154–159.

Mendelson, M., Tekoah, Y., Zilka, A., Gershoni-Yahalom, O., Gazit, R., Achdout, H., Bovin, N.V., Meningher, T., Mandelboim, M., Mandelboim, O., et al. (2010). NKp46 O-glycan sequences that are involved in the interaction with hemagglutinin type 1 of influenza virus. J. Virol. *84*, 3789–3797.

Mishra, B.B., Rathinam, V.A., Martens, G.W., Martinot, A.J., Kornfeld, H., Fitzgerald, K.A., and Sassetti, C.M. (2013). Nitric oxide controls the immunopathology of tuberculosis by inhibiting NLRP3 inflammasome-dependent processing of IL-1β. Nat. Immunol. *14*, 52–60.

Miyake, Y., Asano, K., Kaise, H., Uemura, M., Nakayama, M., and Tanaka, M. (2007). Critical role of macrophages in the marginal zone in the suppression of immune responses to apoptotic cell-associated antigens. J. Clin. Invest. *117*, 2268–2278.

Mosser, D.M., and Edwards, J.P. (2008). Exploring the full spectrum of macrophage activation. Nat. Rev. Immunol. *8*, 958–969.

Müller, U., Steinhoff, U., Reis, L.F., Hemmi, S., Pavlovic, J., Zinkernagel, R.M., and Aguet, M. (1994). Functional role of type I and type II interferons in antiviral defense. Science *264*, 1918–1921.

Naugler, W.E., Sakurai, T., Kim, S., Maeda, S., Kim, K., Elsharkawy, A.M., and Karin, M. (2007). Gender disparity in liver cancer due to sex differences in MyD88-dependent IL-6 production. Science *317*, 121–124.

Pfaffl, M.W. (2001). A new mathematical model for relative quantification in real-time RT-PCR. Nucleic Acids Res. *29*, e45.

Schindelin, J., Arganda-Carreras, I., Frise, E., Kaynig, V., Longair, M., Pietzsch, T., Preibisch, S., Rueden, C., Saalfeld, S., Schmid, B., et al. (2012). Fiji: an open-source platform for biological-image analysis. Nat Methods *9*, 676–682.

Trifilo, M.J., and Lane, T.E. (2004). The CC chemokine ligand 3 regulates CD11c+CD11b+CD8α- dendritic cell maturation and activation following viral infection of the central nervous system: implications for a role in T cell activation. Virology *327*, 8–15.

Vivier, E., Tomasello, E., Baratin, M., Walzer, T., and Ugolini, S. (2008). Functions of natural killer cells. Nat. Immunol. *9*, 503–510.

Wherry, E.J. (2011). T cell exhaustion. Nat. Immunol. *12*, 492–499.

Wilder, J.A., Koh, C.Y., and Yuan, D. (1996). The role of NK cells during in vivo antigen-specific antibody responses. J. Immunol. *156*, 146–152.

Yi, A.-K., Chace, J.H., Cowdery, J.S., and Krieg, A.M. (1996). IFN-gamma promotes IL-6 and IgM secretion in response to CpG motifs in bacterial DNA and oligodeoxynucleotides. J. Immunol. *156*, 558–564.

STAR★METHODS

KEY RESOURCES TABLE

REAGENT or RESOURCE	SOURCE	IDENTIFIER
Antibodies		
Alexa Fluor 647 αB220, clone RA3-6B2	BioLegend	Cat# 103226 RRID:AB_389330
Brilliant Violet 605 αB220, clone RA3-6B2	BioLegend	Cat# 103244 RRID:AB_2563312
PE/Cy7 αB220, clone RA3-6B2	BioLegend	Cat# 103222 RRID:AB_313005
Pacific Blue αCD21/CD35, clone 7E9	BioLegend	Cat# 123414 RRID:AB_2085158
APC/Cy7 αCD4, clone GK1.5	BioLegend	Cat# 100414 RRID:AB_312699
Alexa Fluor 488 αF4/80, clone BM8	BioLegend	Cat# 123120 RRID:AB_893479
APC/Cy7 αF4/80, clone BM8	BioLegend	Cat# 123118 RRID:AB_893477
Alexa Fluor 647 αCD11c, clone N418	BioLegend	Cat# 117312 RRID:AB_389328
APC/Cy7 αCD11c, clone N418	BioLegend	Cat# 117324 RRID:AB_830649
Brilliant Violet 711 αCD11c, clone N418	BioLegend	Cat# 117349 RRID:AB_2563905
Alexa Fluor 647 αCD169, clone 3D6.112	BioLegend	Cat# 142408 RRID:AB_2563621
PE αCD169, clone 3D6.112	BioLegend	Cat# 142404 RRID:AB_10915697
PE/Cy7 αCD3, clone 17A2	BioLegend	Cat# 100220 RRID:AB_1732057
efluor 450 αCD3, clone 17A2	eBioscience	Cat# 48-0032-82 RRID:AB_1272193
Purified αCD16/32, clone 93	BioLegend	Cat# 101302 RRID:AB_312801
APC αCD44, clone IM7	BioLegend	Cat# 103012 RRID:AB_312963
Alexa Fluor 647 αCD19, clone 6D5	BioLegend	Cat# 115525 RRID:AB_493340
APC/Cy7 αCD86, clone GL-1	BioLegend	Cat# 105030 RRID:AB_2244452
PE αCD95/FAS, clone 15A7	eBioscience	Cat# 12-0951-81 RRID:AB_465788
Alexa Fluor 488 αCD11b, clone M1/70	BioLegend	Cat# 101217 RRID:AB_389305
Alexa Fluor 647 αCD11b, clone M1/70	BioLegend	Cat# 101218 RRID:AB_389327
Brilliant Violet 421 αCD138/Syndecan-1, clone 281-2	BioLegend	Cat# 142523 RRID:AB_2565621
PE-Cy7 αCD27, clone LG.7F9	eBioscience	Cat# 25-0271-82 RRID:AB_1724035
FITC αCD69, clone H1.2F3	BioLegend	Cat# 104505 RRID:AB_313108
Alexa Fluor 488 αGL-7, clone GL-7	eBioscience	Cat# 53-5902-82 RRID:AB_2016717
Alexa Fluor 488 αGr-1, clone RB6-8C5	BioLegend	Cat# 108417 RRID:AB_389309
Alexa Fluor 647 αGranzymeB, clone GB11	BioLegend	Cat# 515405 RRID:AB_2566333
Brilliant Violet 650 αI-A/I-E, clone M5/114.15.2	BioLegend	Cat# 107641 RRID:AB_2565975
Pacific Blue αI-A/I-E, clone M5/114.15.2	BioLegend	Cat# 107620 RRID:AB_493527
Goat αIg (H+L)-AP	Southern Biotech	Cat# 1010-04
Goat αIgG biotin	Southern Biotech	Cat# 1030-04
Avidin-Peroxidase	Sigma-Aldrich	Cat# A3151
Brilliant Violet 785 αIFNγ, clone XMG1.2	BioLegend	Cat# 505838 RRID:AB_2629667
PE αLy-6C, clone HK1.4	BioLegend	Cat# 128007 RRID:AB_1186133
Brilliant Violet 711 αLy-6G, clone 1A8	BioLegend	Cat# 127643 RRID:AB_2565971
PE αMHC class I, clone SF1-1.1	BioLegend	Cat# 116607 RRID:AB_313742
APC αIL-6, clone MP5-20F3	BioLegend	Cat# 504508 RRID:AB_10694868
Alexa Fluor 488 αNK1.1, clone PK136	BioLegend	Cat# 108718 RRID:AB_493183
APC αNK1.1, clone PK136	BioLegend	Cat# 108710 RRID:AB_313397
αNK1.1 *InVivo*mAb anti-mouse NK1.1, clone PK136	BioXCell	Cat# BP0036 RRID:AB_1107737
αIFNγ, *InVivo*mAb anti-mouse IFNγ, clone XMG1.2	BioXCell	Cat# BE0055 RRID:AB_1107694
αIL-6, *InVivo*mAb anti-mouse IL-6, clone MP5-20F3	BioXCell	Cat# BE0046 RRID:AB_1107709

(*Continued on next page*)

Continued

REAGENT or RESOURCE	SOURCE	IDENTIFIER
Bacterial and Virus Strains		
Influenza A virus strain A/PR/8/34	Gonzalez et al., 2010	N/A
Vaccinia Virus Strain NYVAC-C	Gómez et al., 2007	N/A
Chemicals, Peptides, and Recombinant Proteins		
Diphtheria Toxin from *Corynebacterium diphtheriae*	Sigma	Cat# D0564
Clodronate Liposomes (CLL) /PBS control liposomes	Clodronateliposomes.com	N/A
Zombie Aqua Fixable Viability Kit	BioLegend	Cat# 423101
Paraformaldehyde powder, 95%	Sigma	Cat# 158127-500G
Agarose, low gelling temperature	Sigma	Cat# A9414
Tween20	Sigma	Cat# 9005-64-5
Triton-X	Sigma	Cat# 9002-93-1
Bovine Serum Albumine (BSA)	Amresco	Cat# 0332
Recombinant Mouse IFN-β Protein	R&D Systems	Cat# 8234-MB-010
Recombinant Mouse IFN-γ Protein	Abnova	Cat# P4450
LPS RB-Ultrapure	InvivoGen	Cat# tlrl-eblps
DiD	Thermo Fisher	Cat# D7757
Ketamin Labatec	Labatec Pharma	Cat# 7680632310024
Rompun 2% (Xylazin)	Bayer	Cat# 6293841.00.00
3-Amino-9-ethylcarbazole	Sigma-Aldrich	Cat# A6926
Critical Commercial Assays		
Intracellular Fixation & Permeabilization Buffer Set	eBioscience	Cat# 88-8824-00
LEGENDplex Mouse Proinflammatory Chemokine Panel (13-plex)	BioLegend	Cat# 740451
LEGENDplex Mouse Inflammation Panel (13-Plex)	BioLegend	Cat# 740150
Experimental Models: Organisms/Strains		
C57BL/6	Janvier Labs	RRID:MGI:5752053
IFNAR$^{-/-}$ mice	Müller et al., 1994	N/A
CD169^{DTR} mice	Miyake et al., 2007	N/A
IFNγR$^{-/-}$ mice	Huang et al., 1993	N/A
Ncr1-GFP mice	Gazit et al., 2006	N/A
OT-II TCR mice	Barnden et al., 1998	N/A
IL-1R$^{-/-}$ mice	Glaccum et al., 1997	N/A
CXCR3$^{-/-}$ mice	Hancock et al., 2000	N/A
Oligonucleotides		
IL-18 FW (5′-GGTTCCATGCTTTCTGGACT-3′)	Microsynth	N/A
IL-18 RV (5′-GGCCAAGAGGAAGTGATTTG-3′)	Microsynth	N/A
IL-6 FW (5′-AGCCAGAGTCCTTCAGAG-3′)	Microsynth	N/A
IL-6 RV (5′-GGAGAGCATTGGAAATTG-3′)	Microsynth	N/A
IFNγ FW (5′-GAGGAACTGGCAAAAGGATG-3′)	Microsynth	N/A
IFNγ RV (5′-GCTGATGGCCTGATTGTCTT-3′)	Microsynth	N/A
IL-1β FW (5′-TGTTTTCCTCCTTGCCTCTG-3′)	Microsynth	N/A
IL-1β RV (5′-GCTGCCTAATGTCCCCTG-3′)	Microsynth	N/A
GAPDH FW (5′-ACATCATCCCTGCATCCACT-3′)	Microsynth	N/A
GAPDH RV (5′-AGATCCACGACGGACACATT-3′)	Microsynth	N/A
Software and Algorithms		
FlowJo software (TriStar , version 10.1)	https://www.flowjo.com/	RRID:SCR_008520
FIJI software (Schindelin et al., 2012, version 1.48k)	https://fiji.sc/	RRID:SCR_002285
Imaris software (Bitplane, version 8.4.2)	http://www.bitplane.com/	RRID:SCR_007370

(*Continued on next page*)

Continued

REAGENT or RESOURCE	SOURCE	IDENTIFIER
LEGENDPlex software (Biolegend, version 7.0)	https://www.biolegend.com/legendplex/software	N/A
Prism software (GraphPad, version 4)	https://www.graphpad.com/scientific-software/prism/	RRID:SCR_002798
Adobe Illustrator (CC2018)	https://www.adobe.com/	RRID:SCR_014198

CONTACT FOR REAGENT AND RESOURCE SHARING

Further information and requests for resources and reagents should be directed to and will be fulfilled by the Lead Contact, Santiago F. Gonzalez (santiago.gonzalez@irb.usi.ch).

EXPERIMENTAL MODEL AND SUBJECT DETAILS

Mice

Mice were bred in house or acquired from Janvier labs (C57BL/6). The following transgenic strains were used: IFNAR$^{-/-}$ (Müller et al., 1994), CD169^{DTR} (Miyake et al., 2007), IFNγR$^{-/-}$ (Huang et al., 1993), *Ncr1*-GFP (Gazit et al., 2006), OT-II TCR (Barnden et al., 1998). IL-1R$^{-/-}$ (Glaccum et al., 1997), CXCR3$^{-/-}$ (Hancock et al., 2000). All strains had C56BL/6 background. For all the experiments young and healthy female mice between 5-7 weeks of age were used. Mice were maintained in specific pathogen-free facilities at the IRB. Experiments were performed in accordance with the Swiss Federal Veterinary Office guidelines and animal protocols were approved by the local authorities.

In vitro NK cell culture and IFN-β stimulation

NK cells were sorted by FACSAria as CD3- NK1.1+ cells from spleens of C57BL/6 female mice and cultured at 5x10^5 cells/ml in complete RPMI with/without rIFN-β 25 pg/well and/or UV-PR8 10^4 PFU/well in 96-well round bottom plates. 12 h later NK cells were surface and intracellular labeled for FACS analysis.

In vitro CD11b+ DC culture and IFNγ stimulation

Splenic CD11c+ DC were purified by magnetic cell separation according to manufacturer's instructions (Miltenyi Biotec). Pre-enriched cells were sorted by FACSAria as CD11c+ MHC-II+ CD11b+ cells and 5x10^5 splenic CD11b+ DC were plated/well into a 96-well plate in complete RPMI alone or with recombinant IFNγ (rIFNγ) (10 μg/ml) or LPS (200 ng/ml) for 12 h. The supernatant was then taken and analyzed for cytokine production.

METHOD DETAILS

Virus production, inactivation and labeling

Influenza virus strain A/PR/8/34 and vaccinia virus strain NYVAC-C (Gómez et al., 2007) were used in this study. Influenza virus was grown for 2 days in the allantoic cavity of 10-day embryonated chicken eggs. In order to remove cellular debris, allantoic fluid was harvested and centrifuged at 3000 rpm for 30 min and virus was subsequently purified twice in a discontinuous sucrose gradient at 25,000 rpm for 90 min. The virus pellet was resuspended in PBS and aliquots were stored at −70°C. Virus stocks were quantified by plaque assays. The vaccinia virus NYVAC-C, provided by Prof. Mariano Esteban, (CNB, Madrid). To inactivate both viruses, viral suspensions were placed under the UV lamp at a distance of 15 cm for 15 min. For the labeling of UV-inactivated influenza virus, 50 μg/ml of DiD was added to the viral suspension and incubated for 20 min at RT. After that, virus was subsequently purified by centrifugation as mentioned before. DiD-UV-inactivated virus aliquots were stored at −70°C.

Antigen administration and injections

10^6 plaque-forming units (PFU) of inactivated virus per footpad in a final volume of 10 μL were injected into anaesthetized mice at different time points prior to LN collection. For macrophage depletion, mice were injected with 10 μl/footpad of CLL or PBS-containing liposomes (control) (Clodronateliposomes.org) at days 5 and 3 before vaccination. Macrophage depletion from CD169^{DTR} mice was established by intraperitoneal (i.p.) injection of 30 ng of diphtheria toxin (Sigma-Aldrich) per g of mouse a day before vaccination. For NK cell depletion 300 μg of αNK1.1 (clone PK136; BioXCell) was administered i.p. (day-3) and intravenously (i.v.) (day-1) before vaccine administration. IFNγ blocking was performed by i.v. injection of 200 μg of αIFNγ (clone XMG1.2, BioXCell) at the time of vaccination. 4 h after vaccination 70 μg / footpad of αIFNγ was administered in a total volume of 10 μl. αIL-6 (clone ALF-161, BioXCell) was administered i.v. at a dose of 200 μg/mice, as well as footpad at 120 μg/mice, at the time of vaccination. For *in vivo* labeling of

cells, mice received 1 μg of fluorescently labeled αCD21/35, αF4/80 and αCD169/footpad (Biolegend), 3 to 5 h before image acquisition.

Flow cytometry

Popliteal LNs were collected, disrupted with tweezers, and digested for 10 min at 37°C in an enzyme mix composed of DNase I (0.28 mg/ml, Amresco), dispase (1 U/mL, Corning), and collagenase P (0.5 mg/mL, Roche) in calcium- and magnesium-free PBS (PBS-) followed by a stop solution composed of 2 mM EDTA (Sigma-Aldrich) and 2% heat-inactivated filter-sterilized fetal calf serum (Thermo Fisher Scientific) in PBS- (Sigma-Aldrich). Fc receptors were blocked (αCD16/32, Biolegend) followed by surface staining and analyzed by flow cytometry on an LSRFortessa™ (BD Biosciences). Where indicated, intracellular and/or nuclear staining was performed according to the instructions (#88/8824/00, eBioscience, #00-5523-00, eBioscience). Dead cells were excluded using ZombieAcqua fixable viability dye (Biolegend) and data were analyzed using FlowJo software (TriStar Inc).

Immunohistology/microscopy

Mice were anesthetized with a mixture of ketamine (100 mg/kg bodyweight, Parke Davis) and xylazine (10 mg/kg bodyweight, Bayer) and perfused with a fixative solution made of 10 mL of 0.05 M phosphate buffer containing 0.1 M L-lysine, 4% paraformaldehyde (PFA), and 2 mg/mL NaIO4 at pH 7.4 (PLP). Popliteal LN were collected and further fixed in 4% PFA at 4°C shaking for 4-6 h and embedded in 5% low gelling agarose (Sigma-Aldrich). 50-100 μm sections were cut with Leica VT 1200S vibratome (Leica Microsystems), blocked with proper sera and stained with the indicated antibodies in 0.05% Tween-20 in 0.5% BSA PBS- for two days at 4°C shaking (see antibody section). Immunofluorescence confocal microscopy was performed using a Leica TCS SP5 confocal microscope (Leica Microsystems). Micrographs were acquired in sequential scans and merged to obtain a multicolor image. Images were processed using Imaris software (Bitplane AG).

Cytoplex assay

LEGENDPlex™ assays (Mouse Proinflammatory Chemokine Panel and Mouse Inflammation Panel; Biolegend) were performed to monitor cytokine/chemokine expression. Briefly, popliteal LNs were collected and carefully disrupted in 100 μL ice-cold phosphate buffer, minimizing cell rupture. The suspension was centrifuged at 1,500 rpm for 5 min, and the supernatant was collected. 25 μL supernatant was used for the protocol following the manufacturer's instructions. Samples were analyzed by flow cytometry on an LSRFortessa (BD Biosciences), and data were analyzed using LEGENDPlex software (BioLegend).

ELISPOT

For enzyme-linked immuno-spot assay (ELISPOT), on day 10 p.v., popliteal LNs were removed aseptically, disrupted, and passed through a 40-μm cell strainer. 4 x10^5 cells were plated on UV-PR8-coated (10^7 PFU/mL) filter plates (MultiScreenHTS, Merck Millipore) and incubated for 16 h at 37°C. For detection, a biotin-conjugated αIgG was used, followed by avidin-Peroxidase (Sigma-Aldrich). A developing solution consisting of 200 mL 3-amino-9-ethylcarbazole (AEC) solution (Sigma-Aldrich) in 9 mL sodium acetate buffer containing 4 mL 30% H_2O_2 was subsequently added. Spots were read on a C.T.L. ELISPOT reader using ImmunoSpot® 5.1 software (Cellular Technology) and counted using ImageJ software.

Multiphoton microscopy and analysis

Deep tissue imaging was performed on a customized two-photon platform (TrimScope, LaVision BioTec). Two-photon probe excitation and tissue second-harmonic generation (SHG) were obtained with a set of two tunable Ti:sapphire lasers (Chamaleon Ultra I, Chamaleon Ultra II, Coherent) and an optical parametric oscillator that emits in the range of 1,010 to 1,340 nm (Cha- maleon Compact OPO, Coherent), with output wavelength in the range of 690–1,080 nm.For the *in vivo* analysis of cell movement, two-photon micrographs were acquired in full Z stacks of 50 μm every 30 s. To analyze NK cell motion quantitatively, manual tracking was used (Imaris 7.7.2, Bitplane). For the statistical analysis of cell migration, only track durations greater than 5 min were considered.

qPCR

Popliteal LNs were collected and disrupted in lysing matrix D 1.4-mm ceramic sphere tubes using FastPrep-24 tissue disruption (MP Biomedicals), and RNA was isolated using an RNAeasy Mini kit (QIAGEN). A final amount of 0.5 μg of cDNA was synthesized using a cDNA synthesis kit (Applied Biosystems) following the manufacturer's recommendations. For qPCR reaction, SYBR Master Mix (Applied Biosystems) was used, and samples were run on a 7900HT Fast Real-Time PCR System (Applied Biosystems). mRNA levels were expressed relative to GAPDH expression. The Pfaffl method (Pfaffl, 2001) was used to calculate the relative expression of the transcripts. Primers: IL-18 FW, 5′-GGTTCCATGCTTTCTGGACT-3′; and IL-18 RV, 5′-GGCCAAGAGGAAGTGATTTG-3′; IL-6 FW, 5′-AGCCAGAGTCCTTCAGAG-3′; IL-6 RV, 5′-GGAGAGCATTGGAAATTG-3′; IFNγ FW, 5′-GAGGAACTGGCAAAAGGATG-3′; IFNγ RV, 5′-GCTGATGGCCTGATTGTCTT-3′ IL-1β FW, 5′-TGTTTTCCTCCTTGCCTCTG-3′; and IL-1β RV, 5′-GCTGCCTAATGTCCC CTG-3′ GAPDH FW, 5′-ACATCATCCCTGCATCCACT-3′;GAPDH reverse, 5′-AGATCCACGACGGACACATT-3′.

QUANTIFICATION AND STATISTICAL ANALYSIS

Statistics

Results were expressed as the mean ± standard deviation (SD). For statistical analysis Prism 4 (Graphpad Software, La Jolla, USA) was used. Data was represented using Prism software. Group comparisons were assessed using nonparametric tests. All statistical tests were two-tailed and statistical significance was defined as: * ($p < 0.05$), ** ($p < 0.01$), *** ($p < 0.001$) **** ($p < 0.0001$). The number of times each experiment was repeated, and the number of animals used per experiment, are detailed in each figure.